ISSN 1070-3632, Russian Journal of General Chemistry, 2015, Vol. 85, No. 5, pp. 1222–1237. © Pleiades Publishing, Ltd., 2015.
Original Russian Text © V.S. Burakov, E.A. Nevar, M.I. Nedel'ko, N.V. Tarasenko, 2013, published in Rossiiskii Khimicheskii Zhurnal, 2013, Vol. 57, Nos. 3–4, pp. 17–30.

Synthesis and Modification of Molecular Nanoparticles in Electrical Discharge Plasma in Liquids

V. S. Burakov, E. A. Nevar, M. I. Nedel'ko, and N. V. Tarasenko

Institute of Physics, National Academy of Sciences of Belarus, pr. Nezavisimosti 68, Minsk, 220072 Belarus
e-mail: burakov.victor@gmail.com

Received January 1, 2013

Abstract—A review of studies on the synthesis and modification of nanosized particles by electrical discharges in liquid media is presented. The modern understanding of the mechanisms of initiation and features of discharge evolution in liquids are analyzed. By using of the spectroscopic diagnostics, parameters of the discharge plasma in liquids (water, ethanol) are determined. It is shown that the pulsed electrical discharge between electrodes immersed in a nonconducting or weakly conducting liquid, provides a simple and effective method for the synthesis of nanoparticles of different compositions with the average size ranging from 5 to 50 nm. The morphology, phase structure, and composition of the particles formed are defined by the discharge mode and composition of the liquid medium in which the discharge is produced. The conditions for the synthesis of nanosized metal oxides, carbides, and silicides (for example, copper and zinc oxides, titanium and tungsten carbides, gadolinium silicides) were found. Zinc oxide nanoparticles were produced in pulsed electrical discharge plasma in distilled water, and the possibility of their doping with nitrogen atoms during synthesis was demonstrated. Experimental results on the modification of tungsten and copper powders by spark discharge in ethanol are discussed. The possibility to synthesize copper chalcogenides $CuInSe_2$ by electrical discharge treatment of a mixture of copper, indium, and selenium powders was demonstrated.

DOI: 10.1134/S1070363215050400

INTRODUCTION

Research into the engineering potential of plasma generated by electrical discharges in liquids or in direct contact with liquids has recently evolved into a new practically important field of plasma physics and chemistry. Immersed or surface discharges are a source of intense UV radiation, shock waves, and radicals and can have useful chemical and biological applications, for example, for disinfection and sterilization. One of the vigorously progressing lines of research in this field is synthesis of nanosized particles in liquids under the action of electrical discharge [1, 2]. As known, nanosized particles and structures hold great promise for application in technology and industry [3–5].

The advantages of the electrical discharge (ED) synthesis of nanoparticles are the possibility to control final product parameters by varying ED parameters, as well as a fairly high performance and the possibility to scale-up the synthesis process, and simplicity of reactor design and preparation of starting materials. Electrical discharge in liquids allows synthesis of a wide range of nanomaterials (metals and intermetallics, nitrides, metal oxides and carbides, composite materials).

Electrical discharge in liquids is accompanied by a complex of physical and chemical phenomena, including shock wave generation, cavitation processes, formation of a vapor–gas bubble and its pulsation, ionization and decomposition of liquid molecules in the plasma channel and around it, intense UV and sound radiation, and pulsed electric and magnetic fields. These processes generate free radicals, singlet oxygen, ozone, and hydrogen peroxide. Furthermore, electrode erosion results in release into the liquid of atoms and ions of the electrode materials. These excited or ionized particles take part in diverse physicochemical processes that affect the liquid and objects placed in it. A great variety of compounds, including metastable ones, can form in the plasma channel. Nanoparticles are formed by chemical reactions of atoms and ions released from electrodes with the decomposition products of the surrounding liquid.

The present paper summarizes the results of research on the formation of molecular nanoparticles in ED plasma in liquids. A number of characteristic approaches to the application of electrical discharge in liquids for the synthesis of nanosized particles of complex composition are considered. The properties of copper oxide and tungsten and titanium carbide nanoparticles, semiconductor nanocrystals (ZnO, $CuInSe_2$), as well as doped zinc oxide nanoparticles, formed in ED plasma in different liquids (water, ethanol, ammonium nitrate solution), are discussed as examples.

Characteristic Features of the Initiation and Propagation of Electrical Discharges in Liquid Media

There is abundant experimental and theoretical evidence to explain the physics of interelectrode breakdown in liquids. The processes that accompany the breakdown in liquids are considered in detail in [6]. According to [6], four mechanisms of discharge initiation (ignition) can be recognized: bubble, microexplosive, ionization, and electrothermal.

The bubble mechanism is realized by breakdown of gas bubbles that are present on the electrodes and in the liquid before discharge ignition.

The mixroexplosive discharge initiation is accompanied by electron emission from the cathode to liquid or by ionization of liquid molecules, which results in local heating of the liquid by electric current. Then a shock wave is formed, whose propagation is accompanied by explosive vapor formation behind its front, ionization of gas–vapor bubbles, and initiation of plasma channel.

The ionization mechanism is operative at very high voltages. The initiation of plasma channel occurs due to ionization of liquid molecules via autoionization or shock ionization. In this case, the energy release, first-order phase transition, and formation of shock waves are secondary processes.

The electrothermal mechanism is realized if voltage is applied for a long time or liquids with high specific electrical conductivities are used. The applied voltage induces boiling up of the liquid and formation of vapor–gas cavities, leading to ionization of gas bubbles inside the cavity. The discharge channel is extended due to motion of the local heating region and boiling-up of liquid toward the opposite electrode.

The discharge propagation stage, too, can occur by different mechanisms [6, 7]: fast, slow, and electrothermal.

The fast (supersonic) mechanism induced by ionization, while the slow (subsonic) mechanism is induced by breakdown of bubbles. The two mechanisms differ from each other only by the intensity and sequence of plasma channel development processes. Both types of discharge affect the phase state of the liquid, and the plasma channel is formed due to gas ionization. It should be noted that, unlike the initiation stage, the discharge maintenance stage is less dependent on the polarity of the initiating electrode.

The electrical breakdown of liquid dielectrics depends on many factors: electrode material, admixtures in the liquid, degassing of the liquid and electrodes, time and rate of voltage rise, and voltage frequency. The electrical type of the breakdown, which develops within 10^{-5}–10^{-8} s, is realized in thoroughly purified liquid dielectrics and is associated with injection of electrons of the cathode [8]. Polar admixtures or gas inclusions induce breakdowns of another type (thermal and ionization), and, therewith, the breakdown voltage drops abruptly [9]. As suggested in [10], even in high electric fields electrons are hydrated and are nearly as mobile as ions. In liquids with ionic conductivity, discharge can be induced only if the discharge gap is very short, and, therewith, discharge is always accompanied by vigorous gas and vapor evolution [11].

The development of discharge in time occurs via consecutive streamer propagation in the inter-lectrode gap [12]. The growth of a streamer from a multitude of plasma channels with branches is likely to be a step discrete process. However, this stepwise character is no longer evident, when the process is considered in whole, because streamer branches grown asynchronously.

Electrical discharge plasma in liquids is non-equilibrium in the sense that electrons have a much higher temperature than the ionic and molecular components. As a result, a great number of collision processes involving electrons are initiated, the main of which are electron impact (EI) ionization and excitation, EI dissociation and dissociative ionization, and ion–atom exchange. The nomenclature of particles involved or formed in elementary processes that take place at the first stage of electrical discharge in water includes molecules, atoms, ions, and radicals: H_2O, H_2, O_2, $^{\bullet}OH$, H, O, O^+, H^+, O^{2+}, OH^-, H_3O^+, etc. [13]. Hydroxyl radicals and hydrogen atoms react with water molecules to form more stable but still chemi-

cally active compounds, such as hydrogen peroxide and ozone, as well as singlet oxygen $^1O_2$, superoxide ion O_2^-, and cluster $H^+ \cdot H_2O$.

The electrical erosion of electrodes occurs because of their heating under bombardment with charged particles. Proponents of another theory argue in favor of the Joule heat released at places where current lines concentrate on the electrode–plasma interface. The release of electrode material into ED plasma is considered in [14].

Analysis of the main physical regularities that control electrical discharge in liquids opens up ways to selecting the most optimal discharge modes for nanoparticle generation.

Development of a Method for Synthesis of Nanoparticles in Electrical Discharge Plasma in Liquids

Bredig and Swedberg [15] were the first to use electrical discharge between metal electrodes immersed in a liquid for preparing colloid solutions of metals [15]. This method was used to obtain organosols of metals, in particular, iron, nickel, cobalt, and their alloys [16] which later found application in chemical catalysis [17].

In the cited works, colloid solutions were prepared by adding fine particles (metal filings) into the liquid where electrical discharge was generated; as a result, arch bridging occurred, accompanied by vigorous dispersion of molten metal to form colloid particles. Under such discharge generation conditions, the degree of metal dispersion was no higher than a few percent, and, therewith, suspensions existed very shortly (about a few minutes), after which particle aggregation and sedimentation took place.

Chiglione and co-workers [18, 19] obtained a uniform suspension using a spark discharge between two metal electrodes immersed in distilled water. Electrical spark dispersion of conducting materials, which allows preparation of their colloid solutions, was used in the determination of major components by atomic absorption spectroscopy [18, 19], as well as microquantities of elements [20] in steels and alloys, but in that time (1970–80s) this method did not find application in the synthesis of nanosized particles.

First works on nanoparticle synthesis with the use of discharge in liquids date back to 1990s. It was shown that the discharge between two metal electrodes in liquid nitrogen [21], ammonia [22], and hydrocarbons [23] results in formation of micro- and nanoparticles of metals and their oxides and nitrides. Therewith, such synthesis does not require complicated vacuum systems, which one of its principal advantages.

In 2000 Ishigami [24] synthesized multilayer carbon nanotubes by means of arc discharge in a liquid. In this work, arc discharge was generated between two graphite electrodes immersed in liquid nitrogen. However, the use of this method was limited by fast evaporation of liquid nitrogen. The replacement of liquid nitrogen by deionized water [25, 26] made it possible to solve it problem and reduced the cost of fabrication of carbon nanostructures. It was found that water and liquid nitrogen fulfill the same functions, specifically, hinder electrode erosion and condensation of erosion products in a limited volume [27]. Moreover, the amount of water evaporated during discharge was found to be much smaller than the consumption of liquid nitrogen [28]. The arc discharge plasma in deionized water was used to synthesize carbon nano-onions and nanotubes similar to those synthesized in liquid nitrogen. At the same time, the nanostructures synthesized in water contain much less defects. Moreover, the nano-onions obtained by this method had a high purity and need not be additionally purified from by-products.

If in the first syntheses be means of electrical discharge in liquids nanoparticles were synthesized from an electrode material, further research focused on the possibility to involve components of the liquid phase in nanoparticle formation.

In 2005 Parkansky et al. [29] reported a series of experiments on the synthesis of nanoparticles in arc discharge in ethanol using carbon, nickel, tungsten, and steel electrodes [29]. The discharge was generated between two electrodes of the same material. The authors of [29] could synthesize nano- and microparticles containing both atoms of the electrode material and carbon atoms (even when the electrodes contained no carbon) formed by the decomposition of ethanol in the discharge zone, as well as various compounds comprising both carbon and metal atoms (intermediate products). The formation of carbon-containing particles suggests that both graphite electrodes and organic liquid (for example, ethanol) can be used as a source of carbon [29]. From the practical viewpoint, the intermediate products are, too,

of great interest. In particular, a way opened up to synthesize tungsten carbide which is applied as a stable and durable material, as well as electrocatalyst [30, 31]. Zheng et al. [32] found that a nanocrystalline tungsten film exhibited catalytic activity in hydrogen reduction reactions.

By the procedure in [29] tungsten carbide formation should necessarily involve atoms generated by the decomposition of the liquid in which the discharge is created, and this obviously adversely affects the efficiency of synthesis of carbide nanoparticles. For a more efficient synthesis of carbide nanoparticles it seems expedient to use pulsed ac spark discharge generated in ethanol between two electrodes, one made of graphite and the second of tungsten.

Of interest also is the phase composition of tungsten carbide powders synthesized under different discharge conditions. According to [33], spark discharge allows more efficient formation of excited atoms and ions from electrode material compared to arc discharge. The use of ac discharge is associated with the necessity to ensure uniform erosion of electrodes made of different materials.

An important application of the ED method is the synthesis of composite nanostructures, in particular, carbon nanostructures decorated by metal particles or carbon-coated metal nanoparticles. Owing to the unique combination of properties of nanostructured wafers and nanoparticles, such composite materials are widely applied in nanoelectronics, as well as a catalysts, chemical sensors, and sorbents for hydrogen storage [4, 34]. Furthermore, magnetic nanoparticles encapsulated in graphite shells are quite attractive for medicine, because the carbon shell, on the one hand, makes it possible to attach substances to be introduced into the body and, on the other, ensures stability of nanoparticles in organic and inorganic liquids and biocompatibility of the introduced particles [3]. The catalytic properties, too, can be much enhanced in composite structures, for example, on deposition of nanoparticles onto carbon nanotubes [4].

Abrams et al. [35] presented a scheme for fabrication of copper-tipped carbon nanotubes, involving the use of mixtures of Fe and Cu particles as catalysts in chemical vapor deposition (CVD synthesis) and growth of nanotubes. Mal'tsev et al. [36] proposed a technology for the synthesis of composite nanoparticles by anode sputtering in an atmospheric pressure electric arc reactor. Metal particles and carbon matrix are formed concurrently, and, therewith, a certain fraction of metal particles are completely encapsulated in carbon structures. Ye et al. [37] reported the deposition of 5–10-nm palladium particles onto multiwalled nanotubes in the reduction of Pd^{II} β-diketonate with hydrogen in the presence of carbon dioxide. Naturally, additional steps on decoration of nanotubes raise the total cost of the final product.

Bera et al. [38] prepared carbon nanotubes decorated by palladium nanoparticles in an arc discharge between two graphite electrodes immersed in a palladium chloride solution. The possibility of synthesis of Ni, Co, and Fe nanoparticles encapsulated in graphite shell by means of arc discharge in aqueous solutions of metal salts ($NiSO_4$, $CoSO_4$, and $FeSO_4$) is demonstrated [39]. Analysis of the chemical composition of the synthesized nanopowder showed that it contained S and O. Decorated carbon nanotubes synthesized in arc discharge in a solution of cobalt sulfate contained not only metal cobalt, but also cobalt sulfide particles [40].

With the development of the electric arc method of synthesis not only electrode materials and working liquids changed, but also the design of discharge generation systems. As a rule, discharge was ignited between two cylindrical electrodes [29, 38], but electrodes having the shape of planar discs with an array of pins (arranged point-to-point) mounted on one of which, or rotating electrodes (one or both) were also reported [41, 42]. Sometimes the working liquid was forced to move [43], which is good for nanoparticle synthesis, because when the liquid is in motion, nanoparticles are removed from the discharge zone, where the temperature is elevated, and stop to grow [43]. Ultrasonication of electrodes during nanoparticle synthesis was used [41]. Certain experiments were performed in so-called hybride reactors, where one electrode was immersed in the liquid and the other was located above the liquid. Discharges are ignited and maintained in different voltage and current modes (direct, pulsed, or alternating current, high- or ultrahigh-frequency current, etc.), and, as a result, a great diversity of plasma conditions are realized.

Experimental Setup for Electrical Discharge Synthesis of Nanoparticles in Liquids

In our experiments on ED nanoparticle synthesis we used a setup comprising four main elements: discharge power source, electrodes, discharge reaction chamber (a glass vessel), and water cooling system (Fig. 1) [44].

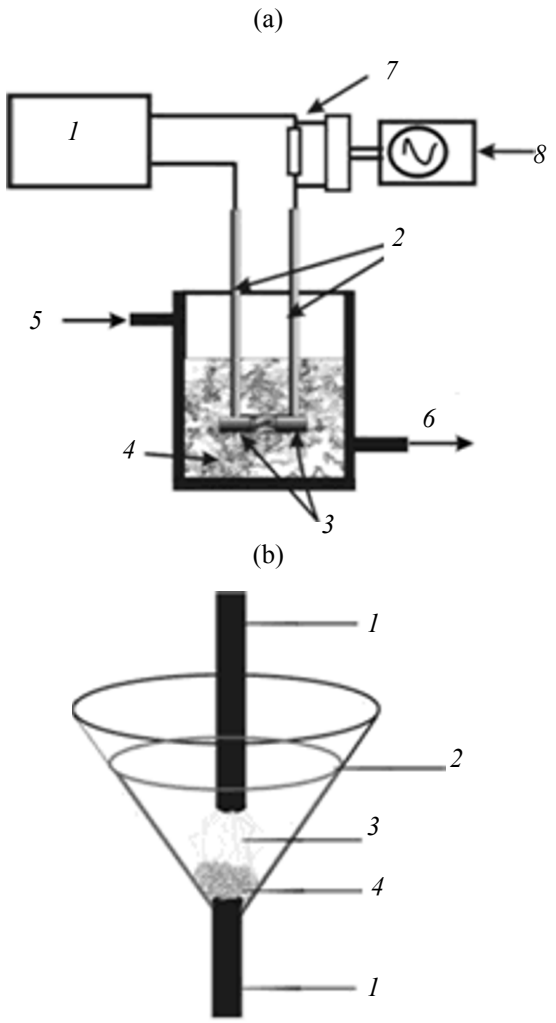

Fig. 1. Schematic diagram of the setup for nanoparticle synthesis under electrical discharge in liquids. (a): (*1*) Power supply, (*2*) electrodes holders, (*3*) electrodes, (*4*) liquid, (*5*) cooled water inlet, (*6*) cooled water outlet, (*7*) current sensor, and (*8*) oscilloscope and (b): (*1*) electrodes; (*2*) cell with ethanol; (*3*) discharge; and (4) treated powder.

To initiate an electrical discharge in a liquid, a power source capable of generating dc and ac currents in the spark or arc modes was used. It is designed for operation from ac power supply with a frequency of 50 Hz and a voltage of 220 V. The high-frequency spark voltage, used to maintain electrical conductivity of the discharge gap, was 3.5 kV. The electrodes, graphite or metal (copper, tungsten, zinc, titanium, etc.) rods 6 mm in diameter, were immersed in the liquid to a depth of 3 cm. The optimal electrode–electrode distance was 0.3–0.5 mm.

The working liquid in the synthesis of tungsten and titanium carbides was ethanol and in the synthesis of zinc oxide, distilled water or aqueous ammonium nitrate. The samples for studies on the catalytic properties of copper were prepared in an aqueous solution of $CuCl_2$ or in ethanol.

In the experiments on ED treatment of powder suspensions we used a different discharge chamber (Fig. 1b). Discharge was ignited between two electrodes, one of which was fixed on the bottom of a cone-shaped vessel loaded with a powder to be treated and the working liquid. The cone shape of the vessel prevented drift of particles from the discharge zone.

The experience acquired during exploitation of the above-described setups was used to develop a pilot laser plasma reactor for fabrication of metal nanopowders and their compounds with widely varied parameters by means of pulsed electrical discharge combined with laser ablation in liquid media. The reactor was equipped by mechanisms for transporting the electrodes to the synthesis zone and for periodically replacing the liquid in the discharge zone. The principal technical characteristics of the reactor and the process of nanoparticle synthesis were as follows: ED source power up to 3 kW; plasma-forming medium liquid or gas; average diameter of the synthesized particles 5–40 nm; deviation from the average diameter ≤30%; and performance up to 50 mg/min.

Determination of the Principal Parameters of the Electrical Discharge Plasma in Liquids

One of the key conditions for successful functioning of ED systems for nanoparticle synthesis in liquids are controlled plasma parameters. The electrical parameters of the discharge are to a large extent responsible for electrode erosion, reaction selectivity, and the presence, along with vapor, of solid or liquid particles in the discharge cloud. Therefore, to know plasma parameters, such as the temperature and concentration of atoms and electrons, is quite important for the optimization of synthesis conditions, especially for the determination of conditions for nanostructure formation (for example, oxides and carbides).

There are only a few reported works focused on the parameters of the ED plasma in liquids in the context of nanoparticle synthesis. In particular, Skibenko et al. [13, 45] made an attempt to measure the density of the ED plasma in water. Microwave probing revealed a correlation between the plasma density rise rate and the rate of EI ionization of particles, thus providing evidence for an ionization breakdown mechanism under that experimental conditions. The experimental decay coefficients of the hydrogen–oxygen plasma in

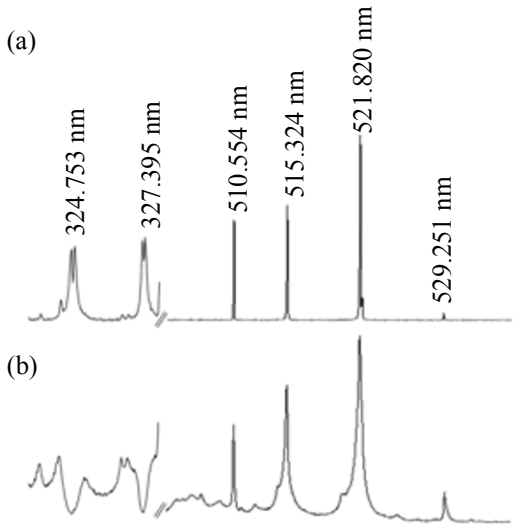

Fig. 2. Typical emission spectra of the plasmas generated by (a) arc and (b) spark discharges between copper electrodes in water.

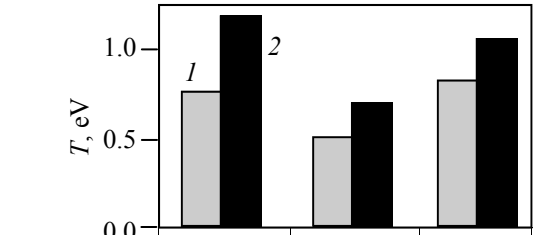

	Water	Air	Ethanol
1	0.77	0.54	0.82
2	1.21	0.74	1.00

Fig. 3. Electron temperatures in electrical discharge plasmas in different media. (*1*) Arc and (*2*) spark.

water were found to be much different from the theoretical values calculated in the framework of the existing nonideal plasma models [46]. These findings provide evidence for the necessity of further diagnostic research on the ED plasma in liquids.

Important information on the parameters of ED plasma can be gained using spectroscopic diagnostic methods [47]. We previously showed [48] that the electron temperature and the concentrations of atoms and electrons can be determined from the plasma emission spectrum.

The spectroscopic studies were performed on the setup in Fig. 1, hyphenated with a spectral instrument, camera for detection of optical emission, photodiode, and other units for measuring the intensity of light signals and their storing and processing. The spectra were registered on a DFS-452 diffraction spectrograph (entrance slit 15 μm, 1200 lines/mm grating for the first-order diffraction) equipped with two CCD arrays. The distance between the arrays can be set for radiation of different wavelengths to be measured simultaneously. Plasma emission was focused with a lens with the focal length of 15 cm. The registration system was controlled from a computer through a USB interface using SSD Tool software.

The emission spectra of the ED plasma in liquids contained spectral lines from atoms and ions of the electrode material and decomposition products of the liquid. As a rule, in the case of arc discharge narrower lines were registered than in the case of spark discharge (Fig. 2).

The parameters of the ED plasma in liquids were much dependent on the peak power of energy deposited into discharge. Notable is a substantial difference in the spectra of the spark and arc discharge plasmas in the region of the resonance lines of electrode material atoms, in particular, CuI 324.753 nm and CuI 327.395 nm. Under the conditions of arc discharge in water, the resonance lines of copper atoms are broadened and self-reversed. In the case of spark discharge, absorption lines were observed in the resonance region instead of emission lines.

From the intensity ratio of the copper lines

CuI 529.251 nm, CuI 521.820 nm, CuI 515.324 nm, CuI 510.554 nm

we estimated the electronic temperature of the plasma: in liquids (water, ethanol) they proved to be slightly higher than in air (Fig. 3).

The electron density of the ED plasma (Table 1) was determined from the H_α line width (Fig. 4).

The concentration of copper atoms in the arc discharge plasma in water, estimated in terms of the inhomogeneous source model, was ~1.1×10^{16} cm^{-3} at the total concentration of atoms and ions of ~6.8×10^{18} cm^{-3}. The spark discharge plasma in water contained about 1×10^{19} cm^{-3} of electrode material atoms.

The component composition of the ED plasma was calculated under the condition of known electron temperature and concentration and in the assumption that the plasma consists of atoms and singly charged ions of the electrode material and the oxygen and

Table 1. Concentrations of electrons in electrical discharge plasma in liquids

Medium	n_e, 10^{-16} cm^{-3}	
	arc	spark
Water	3.2	58.2
Alcohol	4.5	30.8
Air	1.5	2.3

hydrogen atoms formed by water dissociation. According to the calculations, the pressure in the spark discharge plasma channel is about 1.5×10^8 Pa at 14000 K. The effective ionization degree in the discharge channel in water is fairly low (0.2 and 8% for the arc and spark discharges, respectively), but, owing to a high plasma density, the concentration of charged particles is fairly high.

High pressure and temperature in the discharge channel are favorable for various chemical reactions and formation of nanoparticles, including metastable phases, which are hardly accomplished by other methods.

Synthesis Examples of Nanosized Structures in Electrical Discharge Plasma

Metal Oxide Nanoparticles

The character of plasmachemical processes induced by electrical discharge in liquids depends on the reactivity of compounds contained in the electrodes and liquid medium. The most probable reaction to occur under the action of the ED plasma generated between metal electrodes in water and aqueous solutions is oxidation.

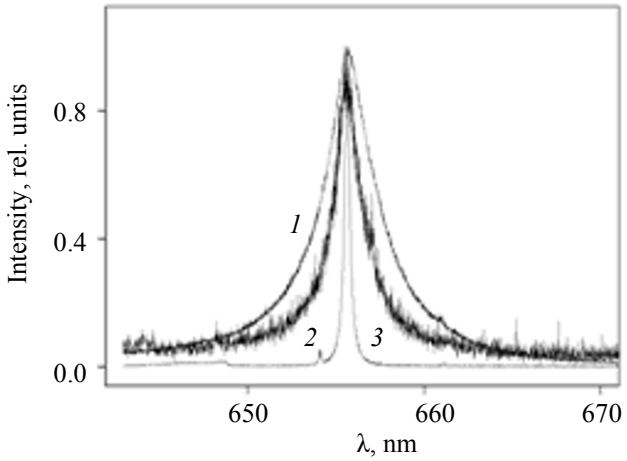

Fig. 4. Profiles of the H_α line registered in spark discharges in (*1*) water, (*2*) air, and (*3*) ethanol.

In [44, 49] we performed a detailed study of the properties of copper oxide nanoparticles, in particular, their catalytic activity in the oxidation of carbon monoxide. Copper oxide nanoparticles were synthesized by the ED method using two graphite electrodes or the pair of a graphite and a copper electrodes. The working liquid was an aqueous solution of copper chloride. Under the conditions of arc and spark discharges, the temperature and concentration of plasma particles in different regimes varied over a fairly wide range. A spark discharge pulse was almost two orders of magnitude shorter compared to an arc discharge pulse. Therefore, the energy power of spark discharge is higher and, as a rule, the rate of particle formation in the spark regime is higher compared to the arc regime. Thus, in the described experiment the average consumptions of electrodes were 9.5 and 4.3 mg/min for spark and arc discharges, respectively.

The parameters of the discharge between the metal–graphite electrode pair have a definitive effect on the morphology of the synthesized nanoparticles. The microscopic images of the samples obtained in the spark discharge plasma show well-defined isolated spherical nanoparticles 3–5 nm in diameter. The diameter of the particles obtained in aqueous $CuCl_2$ varied from 3 to 35 nm, and the diameter of the particles synthesized in ethanol spanned the range ~5–8 nm (Fig. 5).

The nanoparticles synthesized in the ac arc discharge plasma characteristically have a core–shell structure. The core diameters in copper-containing nanoparticles are no larger than 25 nm, and the diameter of shelled particles reaches 50 nm. The metal core of a nanoparticle encapsulated in a graphite shell is formed by reduction of metal ions in solution while the discharge is glowing. The nanoparticle shell is formed from the carbon evaporated from the electrode surface. The synthesis of core–shell nanoparticles in arc discharge is the more efficient the longer electrode erosion products dwell at a high temperature in the chemical reaction zone.

The morphology and phase composition of copper oxide particles depended on discharge conditions, in particular, on the composition of the aqueous solution in which the discharge was generated. Thus, the nanopowder obtained in aqueous $CuCl_2$ comprised Cu_2O (67.8%) and copper (31.4%). The sample

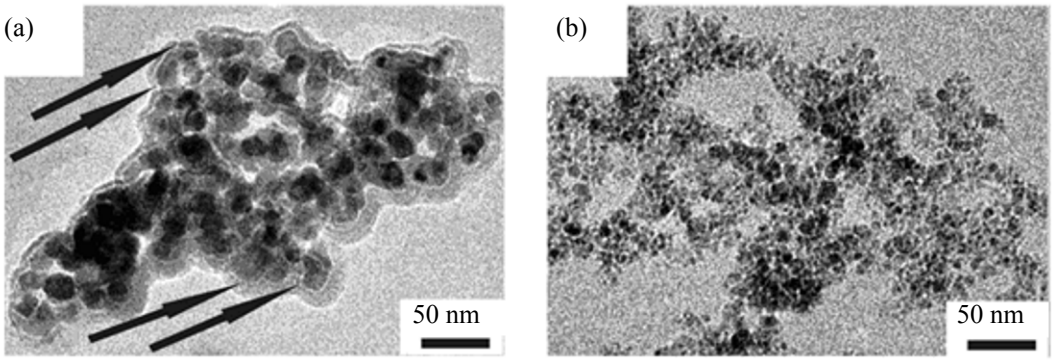

Fig. 5. TEM images of the nanoparticles synthesized under spark discharge in (a) aqueous $CuCl_2$ and (b) ethanol.

synthesized in ethanol contained 69.8% of copper and 30.2% of Cu_2O. In the discharge generated in a copper chloride solution, reactions with chlorine, leading to copper hydroxychloride and oxychloride, are possible. Copper carbide was not found [35].

The morphology, structure, and composition of samples synthesized under different discharge conditions allowed conclusions concerning possible mechanisms of the formation of copper-containing nanoparticles, induced by ED in liquids. The temperature in the discharge zone varies roughly from the boiling point of the electrode material to the boiling point of the liquid at the gas mixture–liquid interface. Thus, the temperature in the discharge zone between copper and graphite electrodes varies from 4000 to 100°C. According to the results of spectroscopic studies, discharge occurs in a gas mixture containing vapors of the working liquid and electrode material. If at least one of the electrodes contains carbon, the gas mixture will contain CO and H_2 formed by the following reaction:

$$C + H_2O \rightarrow CO + H_2. \quad (1)$$

In the case of the discharge between copper and graphite electrodes, copper vapor forms as a result of both erosion of the copper electrode and evaporation and thermal decomposition of the working liquid (aqueous $CuCl_2$). Nanoparticles are formed from atoms and gaseous complexes via consecutive particle nucleation, growth, coalescence, and aggregation. Nanoparticles stop to grow on contact with a colder liquid surrounding the discharge zone. The copper atoms formed by both electrode evaporation and ion reduction most likely trigger this sequence of events. The presence of water vapor in the mixture leads to the formation of oxides which can further be reduced by CO and H_2:

$$Cu_2O + CO \rightarrow 2Cu + CO_2, \quad (2)$$

$$Cu_2O + H_2 \rightarrow 2Cu + H_2O. \quad (3)$$

However, as follows from X-ray diffraction (XRD) data, copper oxide is reduced only partially and under certain discharge conditions.

The nanoparticles synthesized in the discharge between two copper electrodes in ethanol exhibited a high catalytic activity in CO oxidation [56]. The catalytic activity became apparent at 130°C, and at 250°C the CO conversion was 100%. The nanoparticles preserved their catalytic activity multiple uses.

The composition of the nanoparticles formed under electrical discharge between zinc electrodes in distilled water was to a great extent determined by the oxygen concentration in the discharge zone and only slightly varied with current power and discharge pulse duration. As the concentration of oxygen in the discharge zone increased with enrichment of water with dissolved oxygen, the content of structural defects in the synthesized particles tended to decrease until the fraction of zinc oxide in the final product reached almost 100%.

Nanostructured zinc oxide, with its large optical band gap (3.37 eV) [50], is applied in UV low-barrier lasers, field emitters, and other microelectronics. In view of potential applications of nanosized zinc oxide structures [51], of interest is to develop approaches to their controlled synthesis for creating structures with desired properties.

Over the past years a variety of zinc oxide nanostructures, specifically nanoparticles, nanowires, nanoribbons, nanorods, and others, have been synthesized [51]. At present ZnO nanoparticles are most commonly synthesized by chemical vapor deposition [52], molecular epitaxy [53], and vapor deposition with thermal [54, 55], laser [56], or magnetron sputtering [57].

Arc discharge in water was used to synthesize zinc oxide nanowires and nanorods [50, 58]. Pokropivnyi and Kasumov [58] also synthesized ZnO tubes, needles, and tetraneedles ~1 μm in length and up to hundreds nanometers in diameter by means of arc discharge in a vacuum and proposed mechanisms of formation of such structures. Thus, the formation of nanoneedles is preceded by rolling of ZnO sheets into rolls and tubes on the precipitate surface, whereas tetraneedles crystallize and grow from the gas phase and are deposited as a white coating.

The ZnO powders synthesized in our experiments in the spark discharge plasma comprised rod-like grains 25 nm in diameter and 75 nm in length (cf. 40 nm and 130 nm, respectively, in the arc discharge plasma) [59].

The possibility of synthesis of zinc oxide particles doped with nitrogen and indium atoms in the discharge between zinc and indium electrodes immersed into a 0.001 M aqueous solution of ammonium nitrate was demonstrated in [60]. Doped ZnO nanocrystals showed a slight shift of diffraction peaks because of insertion of admixture atoms. Doped ZnO nanoparticles present interest for practice as nanocrystals with hole conductivity, which can be used in semiconductor UV light-emitting diodes.

Metal Carbide Nanoparticles

Titanium and tungsten carbide nanoparticles were synthesized by electric discharge between two metal electrodes in ethanol [61, 62]. The sources of carbon for carbide formation were the products of plasmachemical reactions involving ethanol, which occur in plasma and at the interface between the plasma plume and surrounding liquid. An important factor affecting the yield of the final products is the reaction time between electrode erosion products and medium components. In its turn, the reaction time depends on the residence time of the erosion products between the high-temperature stability limit of the compound and the low-temperature limit, when the reaction rate becomes low.

The temperature in the discharge zone between tungsten electrodes can reach ~5500°C (the melting and boiling points of tungsten are 3422 and 5555°C, respectively). The gas mixture in the discharge zone contains not only vaporized electrode material, but also thermal decomposition products of ethanol [63]:

$$C_2H_5OH \rightarrow C_2H_4 + H_2O, \quad (4)$$

$$C_2H_5OH \rightarrow CH_3CHO + H_2. \quad (5)$$

However, taking into account of the temperature gradient in the near-electrode region, one should expect formation of other ethanol thermolysis products (up to atomic C, H, and O), which are unevenly distributed in the discharge zone. The emission spectra of the discharge plasma in ethanol show, along with lines of electrode material atoms, the line of hydrogen (H_α) and the Swan band system assignable to the C_2 molecule [65]. The hydrocarbons and carbon that are formed react with electrode material atoms to give carbides (W_2C, WC, TiC, TiC_2) [66, 67].

The phase composition of the metal carbides forming in the ED plasma in ethanol depends on the discharge characteristics. Thus, the powders formed in the spark discharge plasma between tungsten electrodes in ethanol, contain WC_{1-x}, W_2C, and C phases (XRD data). In the products obtained in the arc discharge mode, decreased relative contents of carbon and a less carbon-saturated tungsten carbide W_2C and increased WC_{1-x} contents are observed.

To obtain a product containing more carbon than W_2C resulting from the synthesis with two tungsten electrodes, in [62] we replaced one tungsten electrode by a graphite one. In the synthesis under discharge between tungsten and graphite electrode in ethanol, carbide formation involves carbon atoms formed by the decomposition of ethanol and vaporization of the graphite electrode.

The typical images of the tungsten carbide nanoparticles synthesized in ac spark and arc discharges are presented in Fig. 6. The particle size in a freshly prepared solution, averaged over 400 particles is 7 nm. The phase compositions of the synthesized powders are listed in Table 2.

The nanoparticles synthesized in electrical discharge between two titanium electrodes had a spherical shape and were 3–10 nm in diameter. Particle agglomerates were observed. According to semiquantitative estimates, the synthesized powder contained 88.7% of TiC (cubic face centered struc-ture), 4.7% of TiC_2 (simple cubic structure), and 6.6% of carbon (simple hexagonal structure). Thermal treatment decreases the content of carbon in the titanium carbide powder or removes it completely. Free carbon particles can be removed by additionally annealing titanium carbide nanoparticles at 670°C [61].

Note that the only products formed under electrical discharge between titanium and tungsten electrodes in

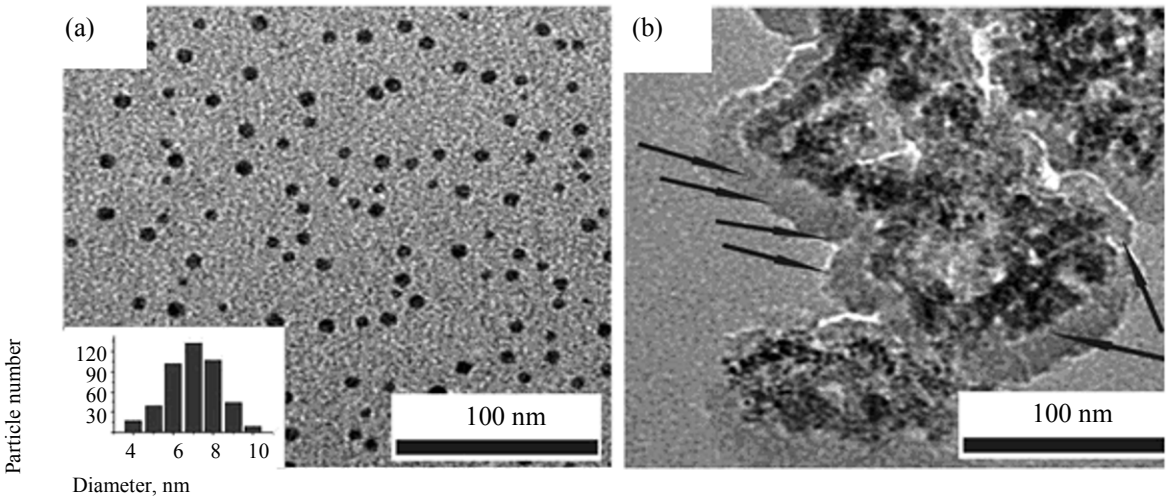

Fig. 6. TEM images of the tungsten carbide nanoparticles synthesized in ac (a) spark and (b) arc discharges. The insert shows the particle size distribution.

ethanol were metal carbide nanoparticles, and no oxide phases were detected.

Titanium and tungsten carbide nanoparticles can be used in durable coatings for metal surfaces of cutting tools. Tungsten carbide nanoparticles synthesized under different discharge conditions can serve as catalysts for hydrogen generation reactions in fuel cells with proton-exchange membranes. The nonstoichiometric tungsten carbide WC_{1-x} is the most efficient among such catalysts. Agglomerates of nanoparticles in graphite shells showed a higher catalytic activity than isolated nanoparticles. High contents of W_2C in nanopowders adversely affect their catalytic activity. Thus, the fields of application of nanostructured tungsten carbide depend on its phase composition [68].

Gadolinium Silicide and Silicon Nanocrystals

The great interest in silicon nanoparticles is associated with their diverse applications. In particular, silicon particles are used in optoelectronics in photocells with enhanced performance and in visible light-emitting devices, in metallurgy as dopants in certain alloys, and biology and medicine as optical probes in cancer diagnostics and therapy.

In [69, 70], silicon nanoparticles were synthesized under electrical discharge between silicon electrodes in distilled water and ethanol. The optical band gaps, estimated by absorption spectroscopy, were 1.7 and 1.56 eV for the silicon nanoparticles synthesized in water and ethanol, respectively, which is much higher

Table 2. Results of X-ray diffraction analysis of the tungsten carbide nanoparticles synthesized under different discharge modes

Electrodes	Types of discharge	R_{Syn},[a] mg/min	Composition and fraction (vol %) of products			
			W_2C	WC_{1-x}	C	W
W : C	ac spark	2.5	5.8	32.8	61.4	–
W : C	ac arc	0.2	7.1	78.1	14.7	–
W(cathode) : C(anode)	dc spark	1.2	57.0	30.7	8.9	3.3
W(anode) : C(cathode)	dc spark	2.1	5.6	32.5	61.8	–
W(cathode) : C(anode)	dc arc	0.1	6.2	90.1	3.7	–
W(anode) : C(cathode)	dc arc	0.2	6.6	71.5	21.9	–

[a] Rate of particle formation.

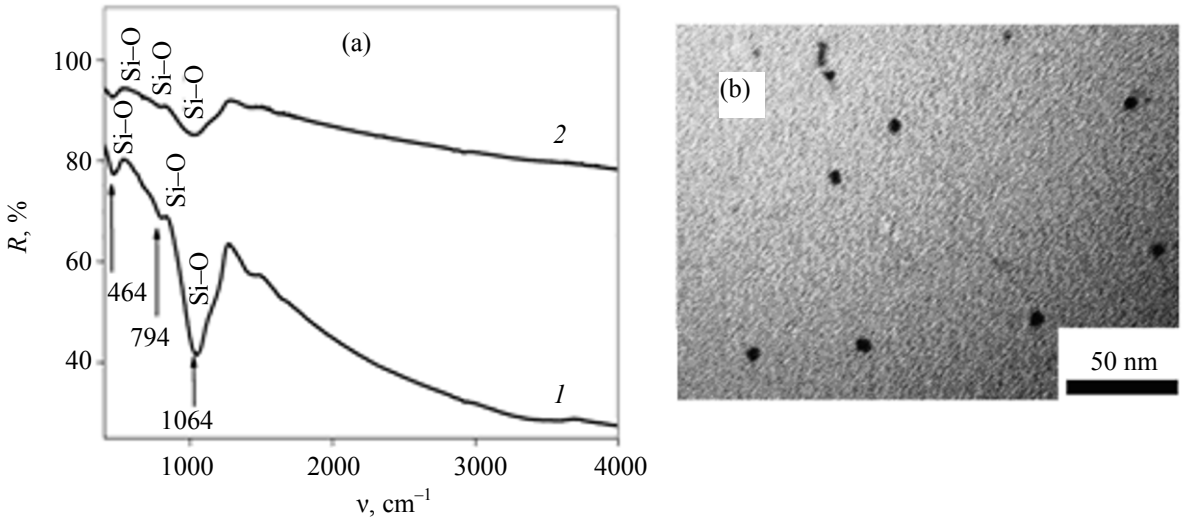

Fig. 7. Fourier transform reflection IR spectrum (a) of the silicon nanoparticles synthesized under electrical discharge in (*1*) water and (*2*) ethanol and (b) TEM image of the silicon nanoparticles synthesized in water.

compared to that of a bulk silicon (1.12 eV [71]) and may be associated with quantum size effects.

The microstructure of the nanoparticles (presence or absence of crystal lattice) was studied by Raman spectroscopy. The spectra showed a shift of the characteristic band of crystalline silicon from its position for a bulk material (520 cm^{-1}). No bands assignable to amorphous silicon were observed, which gave evidence showing that the nanoparticles contained the crystal phase of silicon.

The broad absorption band at 1050–1200 cm^{-1} in the Fourier transform IR spectrum (Fig. 7a) corresponds to characteristic Si–O stretching vibrations [72]. The band near 460 cm^{-1} and a weak band near 800 cm^{-1}, too, correspond to Si–O stretching vibrations [73, 74]. The fact that the sample contains silicon oxide is confirmed by XRD data. The nanoparticles synthesized in water consist of silicon with a cubic structure (85%) and SiO_2 with a monoclinic structure (15%). According to [72], the oxide shell is mainly responsible for the fact that the particles emit light in the visible range. The composition of the nanoparticles synthesized in ethanol is as follows: silicon (95%) and Si_5C_3 (5%).

The luminescence spectra of the silicon nanoparticles synthesized in the discharge plasma in water contained a broad blue band with two characteristic maxima (near 417 and 439 nm), which agrees with data in [73, 75]. The luminescence spectra of colloid solutions of the nanoparticles synthesized in ethanol characteristically showed a broad band with its maximum near 460 nm.

The silicon nanoparticles synthesized in the discharge plasma in distilled water are spherical, and the average particle size is 5.5±0.2 nm (Fig. 7b).

A combination of a silicon and a metal electrodes allows synthesis of silicide nanostructures under discharge in ethanol [76]. Spherical 15-nm Gd_5Si_4 nanoparticles (with minor admixtures of GdSi and Gd_5Si_3) were synthesized. Magnetic measurements showed that the nanoparticles have no hysteresis at a low temperature (6 K), which is characteristic of superparamagnetic nanoparticles.

Modification of Powders in Discharge Plasma in Liquids

A separate application of ED methods is to activate physicochemical processes, in particular, reactivity enhancement of metal and metal compound powders.

Electrical discharge treatment of powders can much affect the kinetics of reaction between particles, decrease the energy of formation of new phases and compounds, increase the surface and bulk diffusion of reacting components, as well as affect the morphological and dimensional characteristics, and, eventually, physical and mechanical properties of final products.

Efficient activation of powders under low-temperature nonequilibrium electrical discharge [77] and high-voltage electrical discharge in liquids was demonstrated [78].

Sizonenko et al. [79, 80] showed that high-voltage electrical discharge in suspensions of Fe–Ti–B_4C and Fe–Ti–C micropowders in a hydrocarbon liquid strongly affects not only the size of particles by splitting them, but also the phase composition of the micropowders. Using a hydrocarbon liquid as the working medium makes it possible to disperse particles without their oxidation, and the carbon that forms can take an active part in solid-phase reactions with powder components to give carbide phases.

In [81] we presented the results of experiments on the modification of tungsten and copper micropowders by spark discharge in ethanol. Electrical discharges were initiated between two graphite electrodes fabricated as rods 6 mm in diameter. The electrode gap was 1.5 cm. The lower electrode was mounted at the bottom of a cone-shaped vessel which was loaded with a powder to be treated and ethanol. The maximum discharge current was 60 A at a discharge pulse time of 30 μs.

To reveal factors influencing the dispersity and phase composition of the final products of ED treatment of metal powders, the results of experiments with mechanically preactivated and nonactivated powders were compared.

The activation of powders by electrical spark discharge occurred under the action of discharge streamers on metal particles of the powder. Therewith, vigorous mixing of the particles took place, because part of them, being raised from the electrode surface by the shock wave generated by collapsing cavitation bubbles, floated up into the liquid volume confined by chamber walls, forming whirlstreams. The appearance of particles suspended in the liquid provides evidence showing that the starting particles have underwent strong fragmentation under ED treatment. One of the possible mechanisms suggests particle heating, melting, and fragmentation in the discharge streamer channels. The reduced particle size is confirmed by the broadening of diffraction peaks after ED treatment.

Along with dispersing the powder, ED treatment in ethanol affects the morphology, phase composition, and crystal structure of tungsten particles. The formation of a new phase (nonstoichiometric tungsten carbide W_3C) and graphite were registered. The most efficient carbide formation was observed with particles that were no mechanically preactivated (the fraction of particles suspended in the liquid). With the mechanically pretreated power, a more efficient carbon shell formation on the particle surface took place.

Unlike tungsten, copper is readily oxidized and does not form carbides. Therefore, in our experiments, the main products of ED treatment of copper micropowder were copper oxides. The new phases are suggested to have a great impact on the structure and properties of materials formed by consolidation of activated powders, in particular, improve their mechanical characteristics.

It should be emphasized that using the ED plasma in multicomponent reactive media one can synthesize nanoparticles of complex phase and chemical compositions. Thus, in our works [82, 83] on ED modification of a mixture of copper, indium, and selenium powders formation of certain copper chalcogenides was detected.

Semiconductor nanomaterials, in particular, $CuInSe_2$ (CIS) and its solid solutions $Cu(In,Ga)Se_2$ (CIGS), are considered as the most promising candidates for application in photovoltaic devices in view of the high absorptivity, good photostability, low toxicity, and a fairly low cost [84, 85]. Since the synthesis of CIS structures for solar cells is fairly complicated and requires controlled joint evaporation of several elements with the use of toxic reagents (H_2Se), over the past years attention has been paid to alternative approaches, in particular, those involving formation of CIS nanocrystal suspensions which can be readily precipitated by centrifuging or jet printing.

As the properties, including optical properties of $CuInSe_2$ nanoparticles are critically dependent on their stoichiometric composition, structure defects, the state of the surface, and the size and shape of the particles, special attention should be paid to the choice of a preparation method.

In [82, 83], $CuInSe_2$ nanocrystals were obtained by treatment of a stoichiometric mixture of copper, indium, and selenium micropowders in a discharge chamber (Fig. 1b). A pulsed spark discharge was initiated between molybdenum electrodes in ethanol. Because the high melting point of molybdenum and its fairly low activity, the treated mixture contained almost no electrode erosion products. The power supply unit generated pulsed discharge with a peak current of 60 A, pulse time of 30 μs, and frequency of 100 Hz. The optimal electrode gap of about ~1 cm was maintained constant to ensure a stable discharge.

To prevent formation of intermediate phases ($CuSe_2$ and In_4Se_3), the CIS nanopowders obtained by

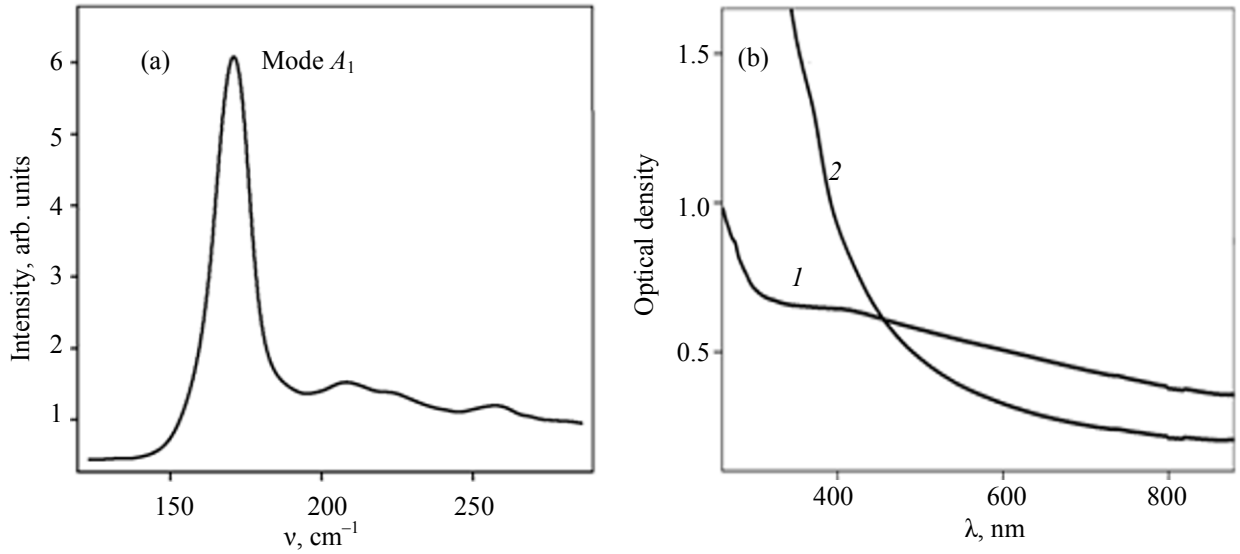

Fig. 8. Typical (a) Raman and (b) absorption spectra of the $CuInSe_2$ nanoparticles synthesized from a stoichiometric mixture of the starting powders under (*1*) arc and (*2*) spark discharges.

ED treatment were annealed in a vacuum for 1.5 h at 700°C.

According to TEM data, the synthesized $CuInSe_2$ nanoparticles were spherical and 20–30 nm in diameter.

The Raman spectrum of annealed nanoparticles (Fig. 8a) contains a band at 172 cm^{-1}, assignable to the optical phonon mode of A1 symmetry. This is the most intense band, and it is usually observed in the Raman spectra of compounds with the chalcopyrite structure [86]. The A1 mode is associated with the motion of Se atoms in CIS, and it differentiated the α-CIS phase with the chalcopyrite structure from the β-CIS phase (182 cm^{-1}) with the sphalerite structure. The weak bands at 208 and 258 cm^{-1} can be assigned to In_4Se_3 and Cu_xSe, respectively.

The absorption spectrum of $CuInSe_2$ nanoparticles contains, as a rule, a broad shoulder with a long-wavelength tail, whose absorption edge is shifted blue compared to a bulk material whose absorption band edge is near 1200 nm [87].

The absorption spectral patterns of the $CuInSe_2$ nanoparticles synthesized by arc or spark discharge treatment of a stoichiometric mixture of powders are much dependent on synthesis conditions (Fig. 8b). This fact provides evidence to show that synthesis conditions affect the size and, possibly, composition and surface state of nanocrystals, which are responsible for the optical properties of nanoparticles.

The blue shift of the absorption band edge of $CuInSe_2$ nanocrystals compared to the respective band for a bulk material is probably explained by the quantum size effects which are observed under the condition that the average diameter of $CuInSe_2$ nanoparticles is smaller than the Bohr exciton radius of $CuInSe_2$ (10.6 nm) [88]. The appearance of a long-wavelength tail is most likely to be associated with a wide particle size distribution and/or with the presence of the intra-bandgap energy levels. The estimated band gap (1.2 eV) is slightly larger than that for a bulk CIS material (1.04 eV) [89] .

CONCLUSIONS

Pulsed electrical discharge between electrodes immersed in a nonconducting or a weakly conducting liquid provides a simple and an efficient technique for synthesis of nanoparticles of different compositions. The parameters of the synthesized nanoparticles can be controlled by varying the discharge mode and liquid composition, in particular, by combining electrodes fabricated from different materials and different working solutions. This technique holds promise for synthesis of molecular nanostructures, such as ternary copper chalcogenides ($CuInSe_2$), as well as metal oxides, carbides, and silicides.

The properties of the synthesized nanoparticles depend on the properties of the ED plasma, in particular, on the temperature and density of plasma

components. Understanding the regularities in the evolution of the ED plasma in liquids allows optimization of nanoparticle synthesis conditions.

Plasma-activated synthesis of nanosized structures in optically transparent liquid media is a fairly young but rapidly progressing field of research aimed at developing a broad spectrum of practical applications, in particular, improving the physical and chemical properties of composite materials. New applications in medicine, electronics, catalysis, optics, and biophotonics are expected.

ACKNOWLEDGMENTS

The work was performed in the framework of the State Program for Scientific Research under project Convergence 2.6.04 and financially supported in part by the Belarusian Foundation for Fundamental Researches (projects F13K-086, F14SRB-008, and F15MC-024).

REFERENCES

1. Takai, O., *Pure Appl. Chem*., 2008, vol. 80, no. 9, pp. 2003–2011.
2. Graham, W.G. and Stalder, K.R., *J. Phys. D: Appl. Phys*., 2011, vol. 44, p. 174037.
3. Bystrzejewski, M., Huczko, A., and Lange, H., *Sens. Actuators B*, 2005, vol. 109, pp. 81–85.
4. Manzoli, M. and Boccuzzi, F., *J. Power Sources*, 2005, vol. 145, no. 2, pp. 161–168.
5. Bukhtiyarov, V.I. and Slin'ko, M.G., *Russ. Chem. Rev*., 2001, vol. 70, no. 2, pp. 147.
6. Ushakov, V.Ya., *Izv. Tomsk. Politekh. Univ.: Tekh. Nauki*, 2006, vol. 309, no. 2, pp. 58–63.
7. Naugol'nykh, K.A. and Roy, N.A., *Elektricheskie razryady v vode* (Electrical Discharges in Water), Moscow: Nauka, 1971.
8. Ushakov, V.Ya., *Impul'snyi elektricheskii proboi* (Pulsed Electrical Breakdown), Tomsk: Tomsk. Univ., 1975.
9. *Issledovanie elektricheskoi prochnosti dielektrikov: Metodicheskie rekomendatsii* (Study of the Electrical Stability of Dielectrics: Methodical Recommendations), Shcherbachenko, L.A., Karnakov, V.A., and Marchuk, S.D., Eds., Irkutsk: Irkutsk. Gos. Univ., 2005.
10. Yanshin, E.V., *Dokl. Akad. Nauk SSSR: Tekh. Fiz*., 1974, vol. 214, no. 6, pp. 1303–1306.
11. Yutkin, L.A., *Elektrogidravlicheskii effect* (Electrohydraulic Effect), Leningrad: Gos. Nauch.-Tekh. Izd. Mashinostroitel'noi Literatury, 1955.
12. Yutkin, L.A., *Elektrogidravlicheskii effekt i ego primenenie v promyshlennosti* (Electrohydraulic Effect and Its Application in Industry), Leningrad: Mashinostroenie, 1986.
13. Skibenko, E.I., et al., *Zh. Tekh. Fiz*., 2007, vol. 77, no. 5, pp. 19–22.
14. Afanas'ev, N.V., *J. Appl. Spectr*., 1966, vol. 5, no. 2, pp. 104–108.
15. Bredig, G., *Z. Angew. Chem*., 1908, vol. 22, p. 951.
16. Lunina. M.A. and Novozhilov, Yu.A., *Kolloid. Zh*., 1969, vol. 31, no. 3, pp. 467–470.
17. Artemov, A.V., *Katal. Prom-sti*, 2001, no. 2, pp. 18–23.
18. Chiglione, M., Eljuri, E., and Cuevas, C., *Appl. Spectrosc*., 1976, vol. 30, no. 3, pp. 320–323.
19. Eljuri, E., Lunar, J., and Chiglione, M., *Appl. Spectrosc*., 1979, vol. 33, no. 2, pp. 170–173.
20. Karyakin, V.Yu., Kharlamov, I.P., and Pchelkin, A.I., *Zavod. Lab*., 1988, vol. 54, no. 4, pp. 36–41.
21. Satsuta, T., et al., *Jpn. Inst. Metals*, 1993, vol. 57, no. 3, pp. 296–300.
22. Sato T., et al., *J. Mater. Sci*., 1992, vol. 27, no. 14, pp. 3879–3882.
23. Sato T., et al., *Brit. Ceram. Trans*., 1995, vol. 94, pp. 205–208.
24. Ishigami, M., et al., *Chem. Phys. Lett*., 2000, vol. 319, nos. 5–6, pp. 457–459.
25. Hsin, Y.L., et al., *Adv. Mater*., 2001, vol. 13, pp. 830–833.
26. Sano, N., et al., *Nature*, 2001, vol. 414, pp. 506–507.
27. Choi, Y.C., et al., *Adv. Mater*., 2000, vol. 12, no. 10, pp. 746–750.
28. Alexandrou, I., et al., *J. Chem. Phys*., 2004, vol. 120, no. 2, pp. 1055–1058.
29. Parkansky, N., et al., *Powder Technol*., 2005, vol. 150, pp. 36–41.
30. Levy, R. and Boudart, M., *Science*, 1973, vol. 181, no. 4099, pp. 547–549.
31. Rosenbaum, M., et al., *Angew. Chem*., 2006, vol. 45, no. 40, pp. 6658–6661.
32. Zheng, H., et al., *Electrochem. Commun*., 2005, vol. 7, pp. 1045–1049.
33. Barvinko, G.G., Barbat, A.M., and Dem'yanchuk, A.S., *J. Appl. Spectr*., 1967, vol. 7, no. 2, pp. 117–119.
34. Moon, T., et al., *Electrochem. Solid State Lett*., 2006, vol. 9, no. 9, pp. A408–A411.
35. Abrams, Z.R., et al., *Nanotechnology*, 2007, vol. 18, p. 495602.
36. Mal'tsev, V.A., et al., *Ross. Nanotekhnol*., 2007, nos. 5–6, pp. 85–89.
37. Ye, X.R., Lin, Y., and Wai, C.M., *Chem. Commun*., 2003, vol. 5, pp. 642–643.

38. Bera, D., et al., *J. Appl. Phys*., 2004, vol. 96, no. 9, pp. 5152–5157.
39. Xu, B., et al., *Carbon,* 2006, vol. 44, no. 13, pp. 2631–2634.
40. Hsin, Y.L., et al., *Adv. Mater*., 2001, vol. 13, pp. 830–833.
41. US Patent 7128816, 2006.
42. Chang, H., et al., *Int. J. Adv. Manuf. Technol*., 2005, vol. 26, pp. 552–558.
43. Artemov, A.B., et al., *Vopr. Atom. Nauki Tekh., Ser. Plazm. Elektron. Novye Metody Uskoreniya*, 2008, no. 4, pp. 150–154.
44. Burakov, V.S., Savastenko, N.A., Tarasenko, N.V., and Nevar, E.A., *J. Appl. Spectr*., 2008, vol. 75, no. 1, pp. 114–124.
45. Skibenko, E.I., et al., *Zh. Tekh. Fiz*., 2006, vol. 76, no. 9, pp. 133–135.
46. Fedorovich, O.A. and Voitenko, L.M., *Vopr. Atom. Nauki Tekh., Ser. Plazm. Elektron. Novye Metody Uskoreniya*, 2008, no. 4, pp. 288–293.
47. Bruggeman, P., Verreycken, T., Gonz´alez, M.A., et al., *J. Phys. D: Appl. Phys*., 2010, vol. 43, pp. 124005.
48. Burakov, V.S., Nevar, E.A., Nedel'ko, M.I., Savastenko, N.A., and Tarasenko, N.V., *J. Appl. Spectr*., 2009, vol. 76, no. 6, pp. 856–863; *Tech. Phys.,* 2011, vol. 56, no. 2, pp. 245–253
49. Burakov, V.S., Butsen, A.V., Misakov, P.Y., Nevar, A.A., et al., *Proc. Int. Conf. on Phenomena in Ionized Gases (ICPIG XXVII)*, Prague, Czech Republic, 2007, pp. 637–640.
50. Ho, G.W. and Wong, A.S.W., *Appl. Phys. A*, 2007, vol. 86, pp. 457–462.
51. Wang, Zh.L., *Mater. Today*, 2004, vol. 7, no. 6, pp. 26–33.
52. Haupt, M., et al., *J. Appl. Phys*., 2003, vol. 93, no. 10, pp. 6252–6257.
53. Chen, Y., Bagnall, D., and Yao, T., *Mater. Sci. Eng. B*, 2000, vol. 75, no. 2–3, pp. 190–198.
54. Yao, B.D., Chan, V.F., and Wang, N., *Appl. Phys. Lett*., 2002, vol. 81, pp. 757–759.
55. Burakov, V.S., Butsen', A.V., Misakov, P.Ya., Nevar, E.A., et al., *Trudy II Mezhdunarodnoi nauchnoi konferentsii* (Proc. II Int. Sci. Conf.), Minsk: Belarus. Gos. Univ., 2007, vol. 3, pp. 140–141.
56. Zherikhin, A.N., *Kvant. Elektron*., 2003, vol. 33, no. 1, pp. 975–980.
57. Jeong, S.-H., Kim, B.-S., and Lee, B.-T., *Appl. Phys. Lett*., 2003, vol. 82, no. 16, pp. 2625–2630.
58. Pokropivnyi, V.V. and Kasumov, M.M., *Pis'ma Zh. Exp. Teor. Fiz*., 2007, vol. 33, no. 1, pp. 88–94.
59. Burakov, V.S., Nedel'ko, M.I., Nevar, A.A., and Tarasenko, N.V., *Tech. Phts. Lett.,* 2008, vol. 34, no. 8, pp. 679–681.
60. Tarasenko, N., Nevar, A., and Nedelko, M., *Phys. Status Solidi A*, 2010, vol. 207, no. 10, pp. 2319–2322.
61. Patent Resp. Belarus no. 12301, appl. 13.11.2007; publ. 30.08.2009.
62. Burakov, V.S., Butsen, A.V., Brüser, F., Harnisch, F., et al., *J. Nanopart. Res*., 2008, vol. 10, no. 5, pp. 881–886.
63. Shvets, V.F., *Soros. Obraz. Zh*., 1996, no. 6, pp. 33–40.
64. Park, J., Zhu, R.S., and Lin, M.C.J., *J. Chem. Phys*., 2002, vol. 117, pp. 3224–3231.
65. Tarasenko, N., Nevar, A., Nedelko, M., and Mardanian, M., *Proc. Int. Conf. on Phenomena in Ionized Gases (ICPIG XXX)*, Belfast, Northern Ireland, UK, 2011.
66. *Kratkaya khimicheskaya entsiklopediya* (Consize Chemical Encyclopedia), Knunyants, I.L., Ed., Moscow: Sovetskaya Entsiklopediya, 1961, vol. 1, p. 651.
67. Smithells, C.J., *Tungsten*, London: Chapman and Hall, 1952.
68. Zellner, M.B. and Chen, J.G., *Catal. Today*, 2005, vol. 99, pp. 299–307.
69. Burakov, V.S., Nevar, A.A., Nedelko, M.I., Mardanian, M., and Tarasenko, N.V., *Trudy VII mezhdunarodnoi konferentsii po fizike plazmy i plazmennym tekhnologiyam* (Proc. VII Int. Conf. on Plasma Physics and Plasma Technolories (PPPT-7)), Minsk, Belarus, 2012, pp. 507–510.
70. Mardanian M., Nevar A.A., Tarasenko N.V. *Appl. Phys. A*, 2012, vol. 112, pp. 437–442.
71. Semaltianos, N.G., Logothetidis, S., Perrie, W., Romani, S., et al., *J. Nanopart. Res*., 2010, vol. 12, no. 2, pp. 573–580.
72. Chen, H.-S., Chiu, J.-J., and Perng, T.-P., *Mater. Phys. Mech*., 2001, vol. 4, pp. 62–66.
73. Yang, Sh., Cai, W., Zeng, H., and Li, Zh., *J. Appl. Phys*., 2008, vol. 104, pp. 023516-1–023516-5.
74. Svrcek, V., Mariotti, D., Nagai, T., Shibata, Y., et al., *J. Phys. Chem. C*, 2011, vol. 115, pp. 5084–5093.
75. Yang, Sh., Cai, W., Zhang, H., Xu, X., and Zeng, H., *J. Phys. Chem. C*, 2009, vol. 113, pp. 19091–19095.
76. Tarasenko, N.V., Nedelko, M.I., and Nevar, A.A., *Nanosci. Nanotechnol. Lett*., 2012, vol. 4, pp. 333–337.
77. Mekhtizade, R.N., *Probl. Energetiki*, 2005, no. 2, pp. 49–55.
78. Bogatyreva, G.P., *Sb. Nauch. Trudov "Porodorazrushayushchii i metalloobrabatyvayushchii instrument – tekhnika i tekhnologiya ego izgotovleniya i primeneniya"* (Collected Papers "Rock-Destructive and Metal-Working Instrument—Technics and Technology of Its Fabrication and Application"), 2009, no. 12, section 2, pp. 191–198.

79. Sizonenko, O.N., et al., Abstracts of Papers, *XV Mezhdunarodnoi Nauchoi Konferentsii "Fizika impul'snykh razryadov v kondensirovannykh sredakh"* (XV Inst. Sci. Conf. "Physics of Pulsed Discharges in Condensed Media"), Nikolaev, Ukraina, 2011, pp. 125–128.
80. Sizonenko, O.N., et al., *Sb. Nauch. Trudov, Tematicheskii vypusk: Tekhnika i elektrofizika vysokikh napryazhenii* (Collected Papers, Special Issue: Technics and Electrophysics of Hygh Voltages), 2009, no. 39, pp. 190–198.
81. Burakov, V.S., Tarasenko, N.V., Nedel'ko, M.I., et al., *Fiz. Khim. Obrabotki Mater*., 2012, no. 6, pp. 18–25.
82. Tarasenko, N.V., Nevar, A.A., Nedelko, M.I., and Mardanian, M., Abstracts of Papers, *4th Central European Symp. on Plasma Chemistry (CESPC)*, Zlatibor, Serbia, 2007, pp. 137–138.
83. Mardanian, M., Nevar, A.A., Nedel'ko, M., and Tarasenko, N.V., *Eur. Phys. J.,* 2013, vol. D67, p. 208.
84. Norako, M.E. and Brutchey, R.L., *Chem. Mater*., 2010, 1991, vol. 22, pp. 1613–1615.
85. Chen, H. and Yoo, J.-B., *Mater. Res. Bull*., 2012, vol. 47, pp. 2730–2734.
86. Chen, H., Yu, S.-M., Shin, D.-W., and Yoo, J.-B., *Nanoscale Res. Lett*., 2010, vol. 5, pp. 217–223.
87. Kavcar, N., *Sol. Energy Mater. Sol. Cells*, 1998, vol. 52, nos. 1–2, pp. 183–195.
88. Castro, S.L., Bailey, S.G., Raffaelle, R.P., et al., *Chem. Mater*., 2003, vol. 15, pp. 3142–3147.
89. Guo, Q., Kim, S.J., Kar, M., Shafarman, W.N., et al., *Nano Lett*., 2008, vol. 8, pp. 2982–2988.